JOURNAL OF NEUROPHYSIOLOGY
Vol. 69, No. 3, March 1993. *Printed in U.S.A.*

Smooth Eye Movements Elicited by Microstimulation in the Primate Frontal Eye Field

JACQUELINE P. GOTTLIEB, CHARLES J. BRUCE, AND MARTHA G. MACAVOY
Section of Neurobiology, Yale University School of Medicine, New Haven, Connecticut 06510

SUMMARY AND CONCLUSIONS

1. We electrically stimulated the macaque monkey's frontal eye field (FEF) region to localize and to analyze the smooth pursuit eye movement representation. Rhesus monkeys were trained to fixate stationary spots of light, and trains of stimulation (usually 250–500 ms at 10–100 μA) were applied while the fixation targets remained lit and stationary. This paradigm was used in a total of 485 electrode penetrations through the arcuate sulcus region of six hemispheres in three adult monkeys. Smooth eye movements (SEMs), clearly distinct from saccades, were elicited at 86 sites in 53 of these penetrations. These SEMs had an average peak velocity of 11°/s and an average latency of 39 ms.

2. The initial acceleration and peak velocity of elicited SEMs increased with stimulation intensity at any given site. On the other hand, SEM direction was characteristic of a given stimulation site and did not vary with stimulation intensity. These findings indicate that SEM amplitude is coded by the intensity of neural activity, and SEM direction is coded by the location of this activity within the cortex ("rate" vs. "place" codes).

3. SEMs elicited in the presence of a stationary fixation target (closed-loop conditions) typically reached a plateau velocity early in the stimulation and maintained that velocity throughout most of the stimulation train. However, when retinal slip was eliminated by artificially stabilizing the fixation target on the fovea (open-loop conditions), the electrical stimulation caused the eye to accelerate for longer periods and to attain higher velocities than in the closed-loop condition. Eye velocities obtained at the same site in open- and closed-loop conditions diverged from one another ~100 ms after SEM onset, consistent with the visual latency of the pursuit system. These findings suggest that the FEF primarily conveys an eye acceleration signal, rather than an eye velocity goal, to the pursuit system, and that this signal can be affected by visual retinal errors before effecting the smooth eye movements.

4. SEMs were elicited from a small portion of the arcuate fundus and neighboring posterior bank lying directly posterior to the principal sulcus. Functionally, this SEM region was surrounded by the saccadic FEF and by somatic premotor cortex.

5. Even though ipsilateral, contralateral, and vertical SEMs were elicited, the distribution of SEM directions was skewed toward ipsilateral movements. This tendency was more pronounced for sites in the arcuate fundus, whereas SEMs elicited from the posterior arcuate bank were often directed contralaterally and vertically. These findings are consistent with the predominantly ipsilateral smooth pursuit deficits obtained after FEF lesions involving the arcuate fundus.

6. At some sites, the direction of the elicited SEM changed as a function of initial orbital position. Quantitative analysis revealed that the magnitudes of these orbital perturbations varied continuously across stimulation sites. SEMs elicited in the posterior bank tended to have larger orbital perturbations than those elicited in the arcuate fundus; however, this difference may have reflected the larger stimulation currents that were used at posterior bank relative to fundus sites.

7. These findings show that a restricted periarcuate region located in the arcuate fundus and in the neighboring posterior bank, between the saccadic FEF and the somatic premotor cortex, is likely to be involved in the execution of smooth pursuit. We hypothesize that this region contributes to smooth pursuit initiation and to the specification of smooth eye acceleration.

INTRODUCTION

The primate frontal eye field (FEF) is defined as that portion of the dorsolateral prefrontal cortex from which rapid eye movements can be elicited with low-intensity intracortical microstimulation. Anatomically, this definition corresponds with the tissue along the anterior bank and part of the lip of the arcuate sulcus (Bruce et al. 1985; Huerta et al. 1986, 1987; Stanton et al. 1988), which is also distinguished from neighboring areas by cytoarchitectonic criteria (Stanton et al. 1989). Many observations strongly argue that the FEF is an important component of the saccadic oculomotor system. Thus the rapid movements elicited from this area are indistinguishable from natural saccades (Robinson and Fuchs 1969). Most neurons in this region respond in relation to visually guided saccades (Bruce and Goldberg 1985), and their presaccadic movement fields are in register with the directions of elicited saccades obtained at their sites (Bruce et al. 1985). Finally, lesions of this area can create deficits in the planning and execution of saccades (Bruce and Borden 1986; Deng et al. 1986; Latto 1978), especially when combined with lesions of other structures (Lynch et al. 1986; Schiller et al. 1980).

More recent reports suggest that the FEF also participates in the control of smooth pursuit eye movements, a class of slow, prolonged eye movements distinct from saccades and specialized for foveal tracking of moving visual targets. Thus FEF ablations degrade smooth pursuit gain (Lynch 1987, 1989; MacAvoy et al. 1991) and the ability to track predictively (in anticipation of, rather than in response to visual target motion; Keating 1991; MacAvoy et al. 1991). A region buried in the arcuate sulcus, lying in or near the saccadic FEF, seems to be most critical for smooth pursuit, because destruction of the arcuate fundus is necessary for obtaining pursuit deficits (MacAvoy et al. 1991). Whereas unilateral FEF ablations primarily affect contralateral saccades, they primarily impair smooth pursuit directed ipsilateral to the effective lesion (MacAvoy et al. 1991).

Little is known so far about smooth pursuit physiology in the periarcuate region. In the course of mapping the saccadic FEF, Bruce et al. (1985) reported that microstimulation at several sites deep in the arcuate sulcus elicited

smooth, rather than saccadic eye movements. In the present experiments we used intracortical microstimulation to more completely delineate and localize the periarcuate smooth eye movement (SEM) representation and to analyze the mechanisms underlying this region's possible involvement in smooth pursuit. Our findings show that SEMs can be electrically evoked from a small region in the fundus and posterior bank of the arcuate approximately at the level of the principal sulcus. These SEMs are predominantly, although not exclusively, directed toward the stimulated hemisphere. Several characteristics of the elicited SEMs suggest that the stimulation effects primarily smooth eye acceleration and does not mimic or substitute for a target velocity signal.

Preliminary reports of these experiments have appeared previously (Gottlieb et al. 1991; MacAvoy et al. 1988, 1991).

METHODS

Surgery and animal care

Three adult female rhesus monkeys (*Macaca mulatta*) were prepared for chronic single-neuron recording and microstimulation in aseptic surgical procedures under pentobarbital sodium anesthesia. A search coil for monitoring eye movements (3 turns of Teflon-coated stainless steel wire) was implanted under the conjunctivum of one eye using standard methods (Judge et al. 1980). A craniotomy (2 cm diam) was trephined over the right frontal lobe, and a stainless steel recording chamber was placed over the craniotomy. To secure the implant, stainless steel bolts with flattened heads were run along slots in the skull, with the bolt head under the skull and then secured with nuts above the skull. The chamber, bolts, connector for the search coil, and a steel receptacle for attaching the monkey's head to the monkey chair were bound together with dental acrylic. During 1-2 wk of postoperative recovery, monkeys were given extra fruit and analgesics (pentazocine lactate 5 mg/kg im or oral Tylenol) as indicated. After several months of recording in the right hemisphere, a recording cylinder was placed over the left frontal lobe in a shorter additional surgery.

Behavioral methods

During experimental sessions, the monkeys sat in a primate chair with their heads restrained, facing a gray tangent screen 57 cm in front of them. Visual targets (red lights ~0.5° diam) were back-projected and moved on this screen by an X-Y mirror system. A PDP-11 computer presented the visual targets, rewarded correct behavior, gated the microstimulation trains, and stored the eye movement traces and unit activity. All experiments were conducted in low-level background illumination. During the course of experiments, the monkeys obtained liquid to satiety each day by performing oculomotor tasks and were given limited access to water in their home cages.

The monkeys were trained on a battery of fixation, saccade, and smooth pursuit tasks, and the data presented here derived primarily from two fixation tasks:

STIMULATION DURING FIXATION. The computer presented a stationary spot of light and gated the stimulation trains (typically 250 or 500 ms) after the monkey fixated this target for a variable interval of 0.5–1.75 s (see below for specifics of stimulation parameters). The fixation requirement was relaxed during stimulation; however, the monkey was required to reobtain the target after the end of the stimulation train and fixate it for an additional interval of 0.25–0.5 s, after which the trial was terminated with a juice reward. The fixation target location was determined either by an experimenter-controlled joystick or by a coordinate array specified at the beginning of each experiment. Except for experiments wherein the fixation location was systematically varied to examine orbital perturbations of the elicited movements, this location was generally kept constant during a given experiment, typically near the monkey's primary position.

STIMULATION DURING FIXATION AND STABILIZATION. This task was identical to the fixation task, except that the fixation light was electronically stabilized on the fovea for the entire length of the stimulation train. Several steps were taken to ensure accurate stabilization. *1*) The eye coil calibration was rechecked before each stimulation and stabilization experiment. *2*) All trials began with the target near the center of the screen. *3*) Control trials using zero current were tested. *4*) Trials that showed evidence of calibration errors, such as small saccades made during stabilization, were omitted from the analysis.

Additional data was obtained by stimulating during spontaneous behavior, that is, when the monkey was not performing a task. We did this while directly observing the monkey's eyes and body to establish that the elicited eye movements, monitored in one eye only, were bilateral and conjugate, and to test for elicited skeletal movements. Because eye records taken during spontaneous behavior were often difficult to interpret, little quantitative data from this condition is included in the present paper.

Physiological methods

Horizontal and vertical components of eye position were recorded using the search coil method (Robinson 1963) and differentiated using an analog circuit to obtain horizontal and vertical eye velocity traces. The signals were calibrated while the monkey fixated small lights at different locations on the screen. Position and velocity signals were sampled by the computer at a rate of 500 Hz and stored for off-line analysis.

Single units were isolated, and stimulation was delivered through glass-coated tungsten or Elgiloy electrodes with tip exposures of 10–20 μm (tungsten) or 20–50 μm (Elgiloy) and in vivo impedances of 0.5–2 mΩ at 1 kHz. Stimulation consisted of 75 to 500-ms trains of biphasic (negative-positive) pulse pairs with 0.2-ms duration per pulse and 300-Hz frequency. Current was monitored by measuring the voltage drop across a 1-kΩ resistor in series with the microelectrode. Currents $\leq$100 μA were routinely used during the search for elicited SEM; currents between 100 and 150 μA were used at a small minority of sites.

Sampling of cortical sites

Electrodes were introduced through the intact dura and advanced through the cortex using a Narishige microdrive hydraulic system with a micrometer scale. In *monkeys HN* and *DN*, we positioned electrodes relative to the millimeter grid affixed to the microdrive stage. In *monkey HZ*, we introduced the grid system made by Crist Instrument (Crist et al. 1988). In this system, a plastic grid with 1-mm spacing between holes along each orthogonal axis determined the brain surface coordinates, and the electrode was advanced into the cortex through a guide tube (fine-gauge stainless steel hypodermic tubing) inserted at the desired grid coordinates before each recording session. This system reduced the variability in electrode paths arising from different electrode bends and penetration angles, and it improved the accuracy and reproducibility of penetrations, especially for sites deep in the sulcus.

During each penetration, we recorded neuronal activity and tested microstimulation at intervals of $\leq$0.5–1 mm; we stimulated at intervals $\leq$0.25 mm above and below any site from which SEMs were elicited. At the majority of the SEM sites, we recorded single-

or multiunit activity before stimulation and thus were assured of stimulating the cortical gray and not the underlying white matter.

Histological techniques

Selected sites were marked either by iron deposits (10–14 μA of positive current for 2–3 min through the Elgiloy electrodes) or by electrolytic lesions (20 μA of negative current for 30 s). At the completion of the experiments, each monkey received an overdose of pentobarbital sodium and was perfused transcardially with saline followed by a 1.25% glutaraldehyde-1.0% paraformaldehyde mixture. The brains were sectioned at 40 μm on a freezing microtome. The brain of one monkey (*DN*) was sectioned in the coronal plane; each hemisphere of the other two monkeys was sectioned approximately perpendicular to the arcuate sulcus at its posterior limit, a plane more appropriate for visualizing the sulcal cortex. Every second or third section through the arcuate sulcus region was reacted with ferrocyanide (Perl's reaction) for visibility of the iron deposits, then counterstained with neutral red or cresyl violet.

Eye record analysis

Stored records of eye movements were analyzed on a Micro VAX computer. Horizontal and vertical smooth eye velocity traces were generated by removing saccades and interpolating eye velocity through the saccadic period. Horizontal and vertical smooth eye acceleration traces were generated by differentiating these smooth velocity traces. For each trial, the polar direction of SEM was defined as the arc tangent of the average horizontal and vertical smooth velocities across the stimulation period, and the "peak" SEM velocity was defined as fastest 100 ms of polar velocity. The median polar direction and median peak velocity were then calculated from blocks of 5–15 identical trials.

For selected sets of trials, we also computed "median profiles" of eye velocity and acceleration by *1*) dividing each elicited SEM into 25-ms bins, *2*) measuring the average horizontal and vertical eye velocity and acceleration in each bin, and *3*) for each bin, taking the median velocity and acceleration across a block of trials with identical experimental conditions. Initial eye acceleration was measured by averaging the second, third, and fourth median values (spanning the epoch of 25–100 ms after stimulation onset).

RESULTS

Characteristics of elicited SEM

In this paper, we consider data obtained in a total of 485 electrode penetrations through the periarcuate regions of

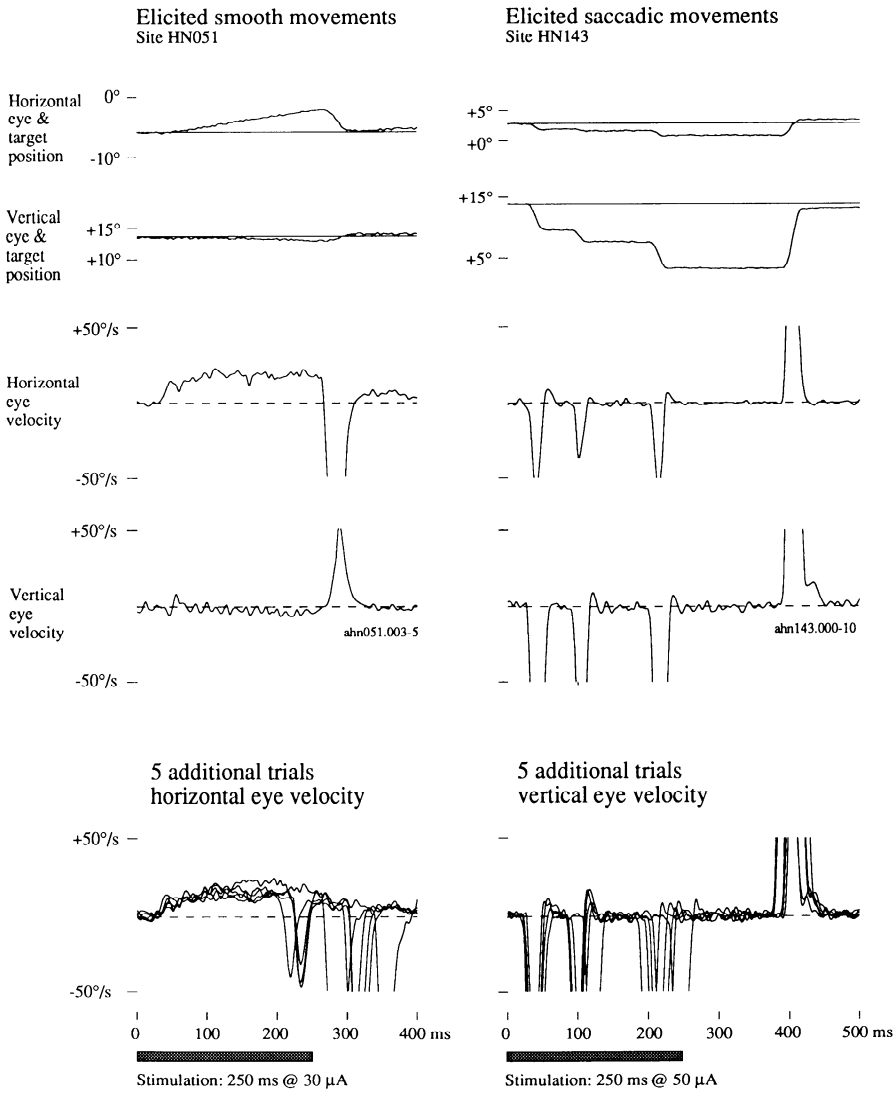

FIG. 1. Smooth and saccadic eye movements elicited at 2 separate sites in the right hemisphere of *monkey HN*. For both the smooth eye movement (SEM) site (*left*) and the saccadic site (*right*), position and velocity traces of 1 trial (first 4 rows) are followed by superimposed velocity traces from 5 additional trials (*bottom* row). All eye velocity traces are truncated at ±50°/s, and for all trials shown, the microstimulation trains (shaded bars) lasted 250 ms. Note the clear distinction between the relatively slow, prolonged SEMs on the *left* and the staircases of much faster, discrete saccades on the *right*. For both position and velocity traces, the positive (upward) deflections represent right or up, and the negative (downward) deflections represent left or down. Note that the elicited SEMs are directed ipsilateral to the stimulated hemisphere. The fixation target remained on throughout the duration of these records and was refixated by voluntary return saccades made after the stimulation train ended. Note the difference in the timing of the refixation saccade for the saccadic and SEM site. Prolonged stimulation at the saccade site appeared to delay the refixation saccade, which seldom occured until 150 ms after the stimulation train ended. In contrast, refixation saccades occured immediately after stimulation at the SEM site and sometimes during the stimulation (*see superimposed traces at the bottom*).

six hemispheres in three rhesus monkeys. SEMs were elicited at 86 different locations ("SEM sites") in 53, or nearly 11%, of these penetrations. (We distinguish between "SEMs" elicited by microstimulation and "smooth *pursuit* eye movements" made when tracking moving targets.)

Figure 1 contrasts typical elicited SEMs with elicited saccades obtained at two separate locations in the right hemisphere of *monkey HN*. As shown in the figure, the elicited SEMs were relatively slow, continuous movements that lasted as long as the stimulation train. In contrast, elicited saccades were fast and brief, similar to natural saccades (Robinson and Fuchs 1969). Prolonged stimulation did not prolong the elicited saccades as it did the elicited SEMs. Instead, it either triggered a single, brief saccade, or produced a staircase of several discrete movements characteristic of the site, as shown in Fig. 1. At 16 of our SEM sites, small, single saccades were also elicited; these saccades typically preceded, and were clearly distinct from, the elicited SEMs.

The distributions of velocities and latencies of elicited SEMs are shown in Fig. 2. Because foveal target stabilization can lead to higher SEM velocities (see below), and because we did not systematically test the effects of stimulating during spontaneous behavior (without a fixation target), only SEMs elicited with the standard stimulation task

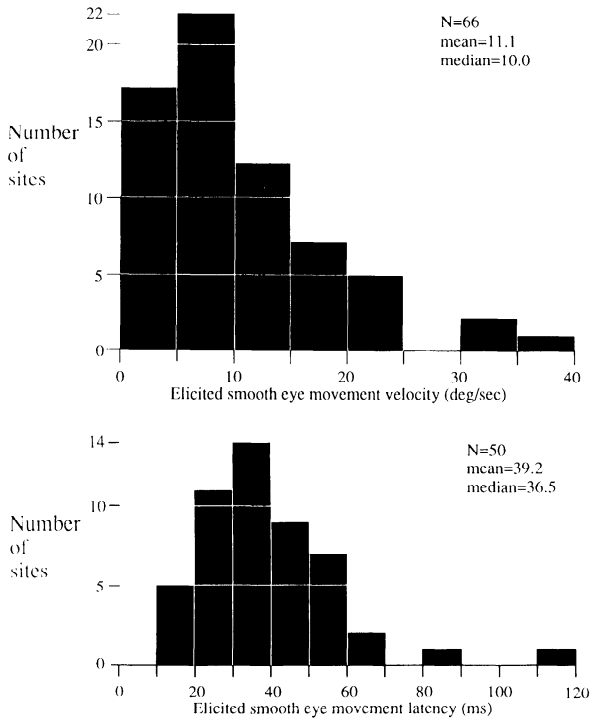

FIG. 2. Elicited smooth eye movement (SEM) velocities and latencies. The distribution of elicited smooth velocities (*top*) and of latencies to the start of the elicited smooth movement (*bottom*) for 66 SEM sites (for selection criteria, see text) are shown. For each site, the best (fastest) set of eye movements obtained with stationary, nonstabilized fixation targets and with currents ≤ 100 μA was used. Velocities are the median across trials of the peak smooth velocity. Latencies (from the onset of the stimulation train) were measured from averaged velocity traces computed from the same sets of records. Sixteen sites where short-latency saccades were elicited along with the elicited SEM were excluded from the latency histogram. The SD of the latency distribution was 17.8 ms.

(in the presence of a stationary fixation target) were included in these histograms. To avoid oversampling, we further excluded sites separated by <0.25 mm along the electrode track. For 64 of the 66 sites thus selected, we chose the best (fastest) sets of SEMs elicited with currents ≤ 100 μA, and at the remaining two sites, we chose records taken with 125 and 140 μA (with eye velocities <7°/s). The velocity distribution thus obtained is skewed toward 5–10°/s, with mean of 11.1°/s and median of 10.0°/s.

We measured SEM latencies from the velocity traces of the averaged eye records of 50 of these 66 SEM sites at which no saccades were also elicited (bottom histogram). Average latency was 39.2 ms after stimulation onset (SD = 17.8).

Dependence of SEM acceleration and velocity on current intensity

In contrast with saccades elicited from the FEF, whose dimensions (velocities, amplitudes, and directions) do not vary much with stimulation intensity (Robinson and Fuchs 1969), the velocities and initial accelerations of elicited SEMs usually increased with current intensity at a given stimulation location. SEM directions, on the other hand, remained constant for a given site over the same intensity ranges. Figure 3 illustrates this finding at one site from the left hemisphere of *monkey HN*. At this location, the horizontal eye velocity and hence the total horizontal excursion monotonically increased with current intensity, whereas vertical velocity remained close to zero for currents between 10 and 75 μA. Elicited movement direction thus remained horizontal, close to 180° (to the left). Fitting the plot of peak eye velocity versus current (last panel) gave a correlation coefficient of 0.95 and a linear regression of $0.27° \cdot s^{-1} \cdot \mu A^{-1}$, indicating an increase of ~7°/s for each 25-μA increment.

The dependence of peak eye velocity on current at 11 SEM sites is shown in Fig. 4, *top*, and the corresponding initial eye accelerations (measured between 25 and 100 ms after stimulation onset) are plotted in the *bottom* part of the figure. For clarity of presentation, sites are divided into those with peak velocities below or above 10°/s ("low"- and "high"-velocity sites). At eight of these sites, experiments were conducted with stationary fixation targets, and at the remaining three (asterisks) fixation targets were stabilized on the fovea during stimulation. Eye velocities increased monotonically at most sites, with correlation coefficients ranging from 0.10 to 0.98 (mean of 0.74) and exceeding 0.70 at all but two of these sites. The average slope of all 11 regressions was $0.13° \cdot s^{-1} \cdot \mu A^{-1}$ (range −0.01 to 0.35) showing that, on the average, eye velocity increased by 3°/s for each 25-μA increment in current intensity. However, the effects of increasing current intensity appeared to diminish with higher currents, particularly at high-velocity sites.

Eye accelerations in most of these experiments also increased with current intensity. At a given site, acceleration and velocity often had similar profiles (corresponding symbols in *top* vs. *bottom* panels in Fig. 4), suggesting that much of the velocity changes were due to changes in the magnitude of the initial eye acceleration. The average lin-

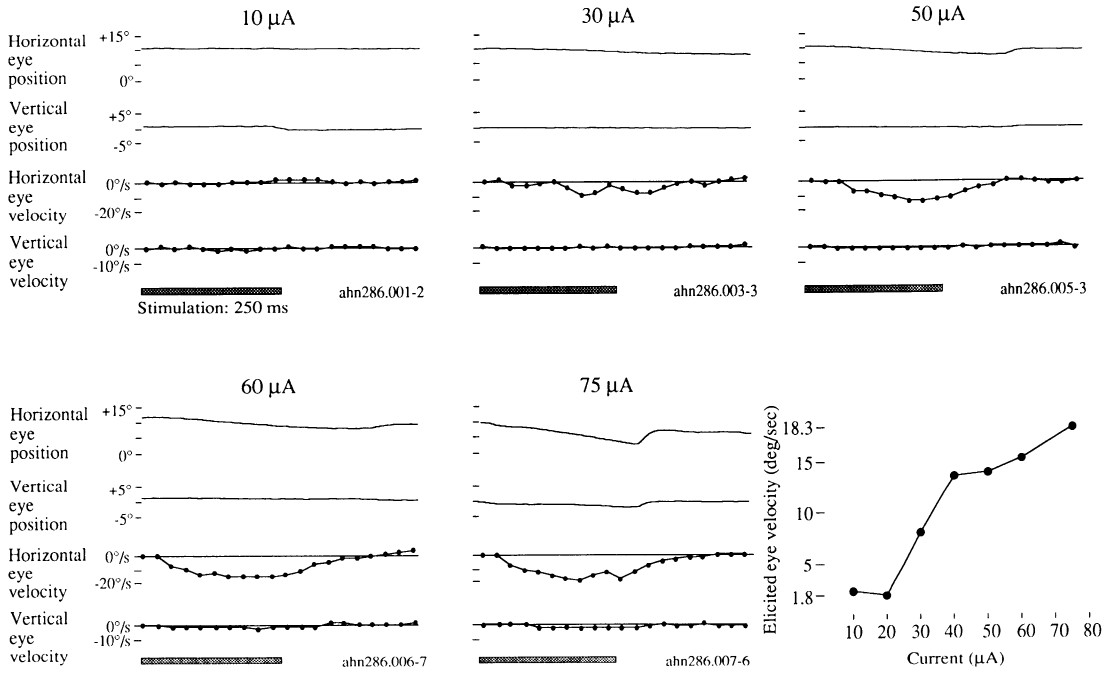

FIG. 3. Effects of current intensity on elicited smooth eye movement (SEM) at 1 site. First 5 panels: eye position traces of representative individual records and "median velocity profiles" (see METHODS) of SEMs elicited at different current intensities. Horizontal (leftward) eye velocity increased with current intensity, whereas vertical velocity remained close to 0, maintaining a constant direction (~180°) for the elicited SEM. Last panel: plot of median peak eye velocity as a function of current intensity. The stimulation site was located in the left hemisphere of *monkey HN*.

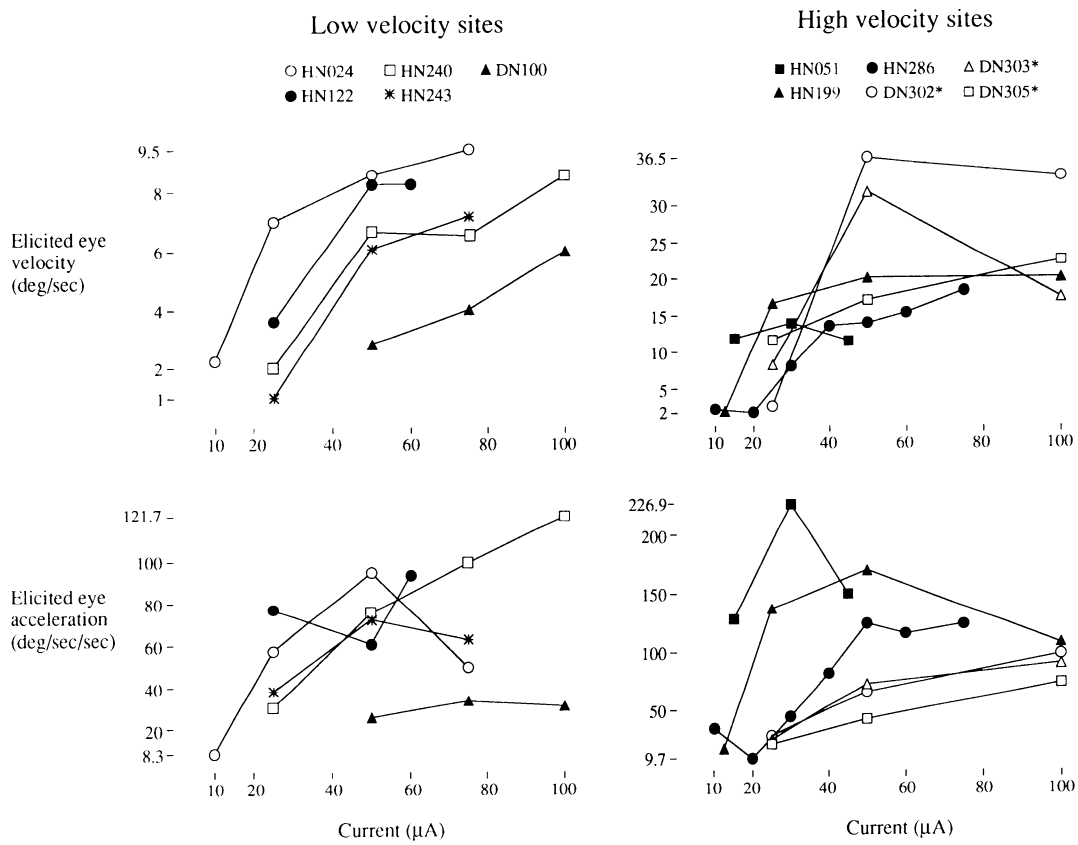

FIG. 4. Effects of current intensity on elicited smooth eye movement (SEM) velocity and acceleration. Median peak eye velocities (*top*) and eye accelerations in the first 75 ms of movement (*bottom*) are plotted for 11 sites tested with different current intensities. Sites are grouped into those with peak eye velocities below and above 10°/s (*left* and *right* columns, respectively). At the 3 sites indicated by asterisks (*right* column), the experiments were conducted with foveally stabilized fixation targets; at all other sites, the fixation targets were stationary.

ear-regression slope across all 11 sites was $0.74° \cdot s^{-1} \cdot \mu A^{-1}$ (range 0.25–1.86), indicating an average increase of $18° \cdot s^{-1} \cdot s^{-1}$ for each 25-μA increment.

The effect of target stabilization on the fovea

The above findings suggest that the FEF contains an intensity-coded signal of either an eye velocity goal or of instantaneous eye acceleration. Whereas the acceleration hypothesis predicts that the eye would continue to accelerate throughout the stimulation train, SEMs elicited in the presence of a stationary fixation target usually reached a plateau velocity well before the end of the stimulation train (see Figs. 1 and 3). In this paradigm, it is possible that the retinal slip (visual motion signal) of the fixation target, which was equal and opposite to the elicited SEM, partially cancelled the electrically induced eye acceleration command and caused a movement with shorter accelerations and lower peak velocities. The plateau velocity could thus represent an equilibrium between the opposing microstimulation and visual signals. To test this hypothesis, we compared the SEMs elicited in the stationary target (nonstabilized) task with those elicited in the stimulation-and-stabilization task, in which the retinal slip was eliminated by stabilizing the fixation target on the fovea during stimulation.

At most sites, target stabilization had profound effects on the elicited SEM, as illustrated in the single trial examples in Fig. 5. At this site, in the nonstabilized condition, the eye reached a peak velocity of 7°/s soon after SEM onset. With the foveally stabilized target, however, the eye continued to accelerate throughout the stimulation epoch and reached a peak velocity of >30°/s. The stabilization did not affect elicited SEM direction, which, in this example, remained down and to the left.

If the target stabilization indeed unmasked an acceleration signal, we would expect to see eye accelerations lasting throughout most of the stimulation-and-stabilization epoch. Further, smooth eye velocities obtained from the same site in the stabilized and nonstabilized conditions should become different from each other at ~100 ms after SEM onset, at approximately the visual latency of the pursuit system. To test these predictions, we compared "median velocity profiles" (see METHODS) obtained in each of the two conditions at the same site. Figure 6 shows the median profiles of horizontal eye velocity (the main velocity component) for five stimulation sites. Consistent with the above predictions, target stabilization usually caused the eye to accelerate longer and to reach much higher velocities relative to the nonstabilized condition. With the exception of site DN303 and possibly DN302, the eye accelerated for as long as the stimulation and stabilization were applied. Eye velocities diverged at the fourth or fifth time bins, or between 75 and 125 ms, at four of the sites shown, and between 50 and 75 ms at site DN302. These observations are consistent with the hypothesis that the electrical stimulation produces mainly a signal of eye acceleration, which is then modified by retinal visual feedback.

Figure 7 compares the peak eye velocities obtained in the

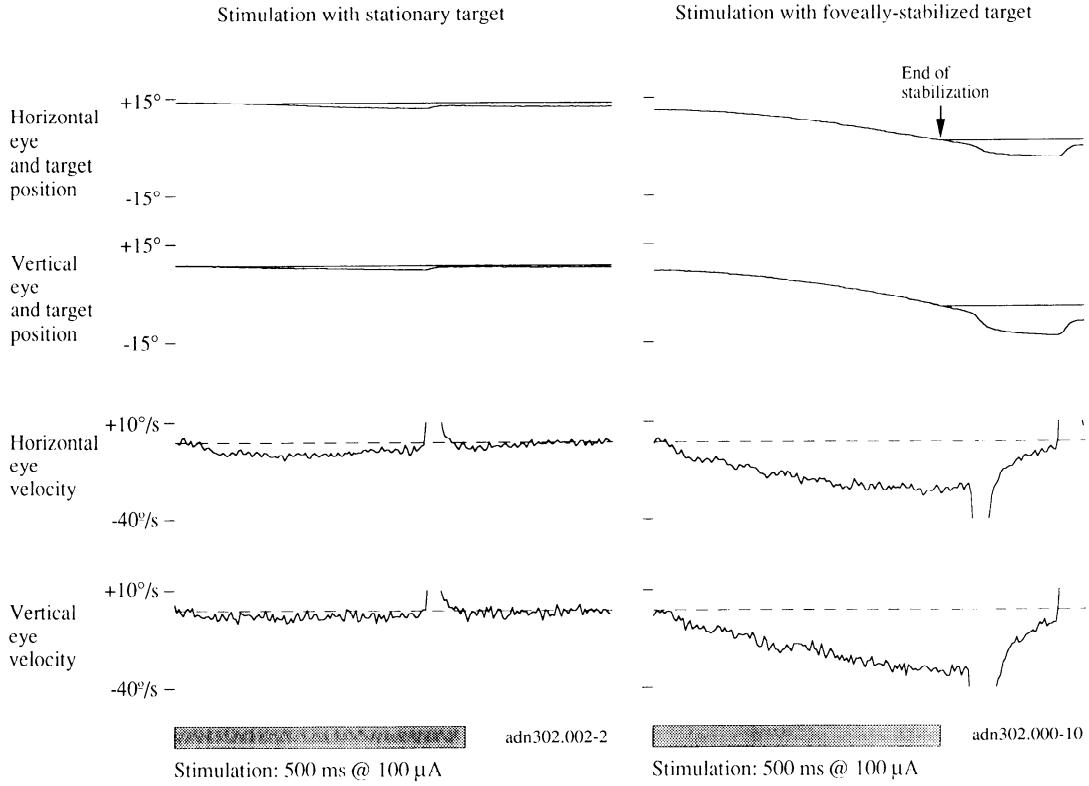

FIG. 5. Effects of foveal stabilization on elicited smooth eye movement (SEM). The eye traces show 1 trial in which stimulation was applied with a stationary fixation target (*left*) and 1 trial with the fixation target foveally stabilized during stimulation delivery (*right*). In the stabilized condition, the eye velocity steadily increased throughout the stimulation and reached much higher values than in the nonstabilized experiment (peak velocities of 30 vs. 7°/s). This stimulation site was located in the left hemisphere of *monkey DN*. Conventions as in Fig. 1.

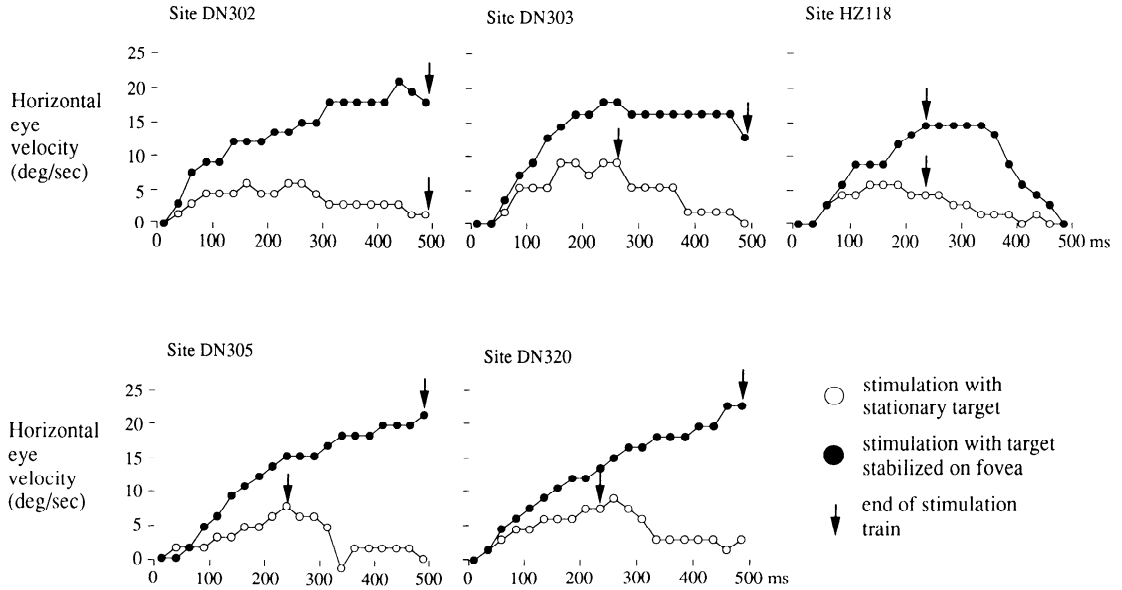

FIG. 6. Median velocity profiles obtained with and without fixation target stabilization. The absolute values of the horizontal (the main) velocity components at 5 sites that showed large effects of stabilization are plotted in each panel; 500 ms of eye movement are always plotted, although the stimulation could last 250 or 500 ms (→). Note that, in most cases, eye velocity continued to increase throughout the stimulation in the stabilized (●) but not in the nonstabilized experiments (○), and that the velocities in the 2 conditions typically diverged from each other between 75 and 100 ms after stimulation onset.

stabilized and nonstabilized conditions at fifteen SEM sites. Each point represents one site, and the abscissa and ordinate represent eye velocities for sets of records obtained without and with target stabilization, respectively. The 45° line illustrates these points' expected distribution had the SEM velocities in both conditions been equal. Stabilization was effective for most sites with nonstabilized eye velocities above ~8°/s, with much smaller effects at sites with lower velocities. This is to be expected if the decrement in eye velocity (and the benefit resulting from stabilization) were related to retinal slip magnitude, which was equal to the elicited SEM velocity in the nonstabilized condition. Elicited eye velocity was not, however, the sole determinant of the stabilization effects, as is seen by the wide range of effects for movements of similar velocities. Other factors in addition to the velocity error signal, perhaps characteristics of a given site, may also influence the effects of target stabilization on the elicited SEM.

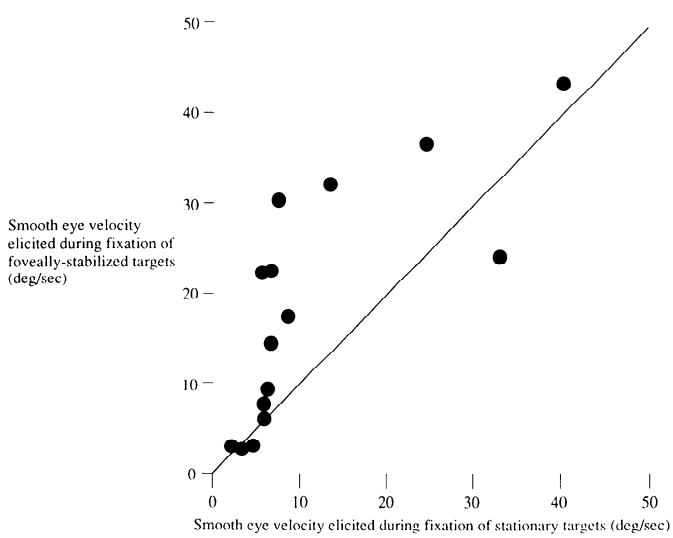

FIG. 7. Eye velocities elicited with and without fixation target stabilization at 15 smooth eye movement (SEM) sites. The ordinate and abscissa coordinates for each site represent the median of the peak eye velocities for tests with and without target stabilization, respectively. Each point was obtained using identical stimulation parameters for both conditions (currents of 50–100 μA, train durations of 250 or 500 ms). The 45° line illustrates the expected distribution if the SEM velocities elicited in both conditions were equal. Note that elicited eye velocities in the stabilized condition surpass those in the nonstabilized condition for most sites in which the nonstabilized velocity was larger than ~8°/s, with little or no difference between the 2 conditions for sites with lower velocities.

Locations of SEM sites

The entry points of all penetrations made in five of the six hemispheres we studied and the elicited movements at each surface coordinate are shown in Fig. 8. These locations were reconstructed with reference to the entry points of penetrations directly identified by iron deposits. (Because of extensive tissue damage, we could not recover the iron deposits made at SEM sites in the right hemisphere of *monkey DN*.) Locations are marked with an × if no eye movements were elicited in any penetration at those coordinates; other symbols indicate coordinates at which ocular—saccadic or smooth—or skeletal movements were elicited in at least one penetration. Saccades were mostly elicited from the anterior, and rarely from the posterior, arcuate banks. Skeletal movements (of the fingers, wrist, arm, shoulder, or face) were sometimes obtained from the posterior banks. SEMs were elicited from penetrations entering both banks within a small area (≤2 × 3 mm in surface projection) located approximately posterior to the principal sulcus in all five hemispheres. In all monkeys, we made repeated penetrations in and immediately around this region. At many coordinates marked as SEM in the anterior banks, we

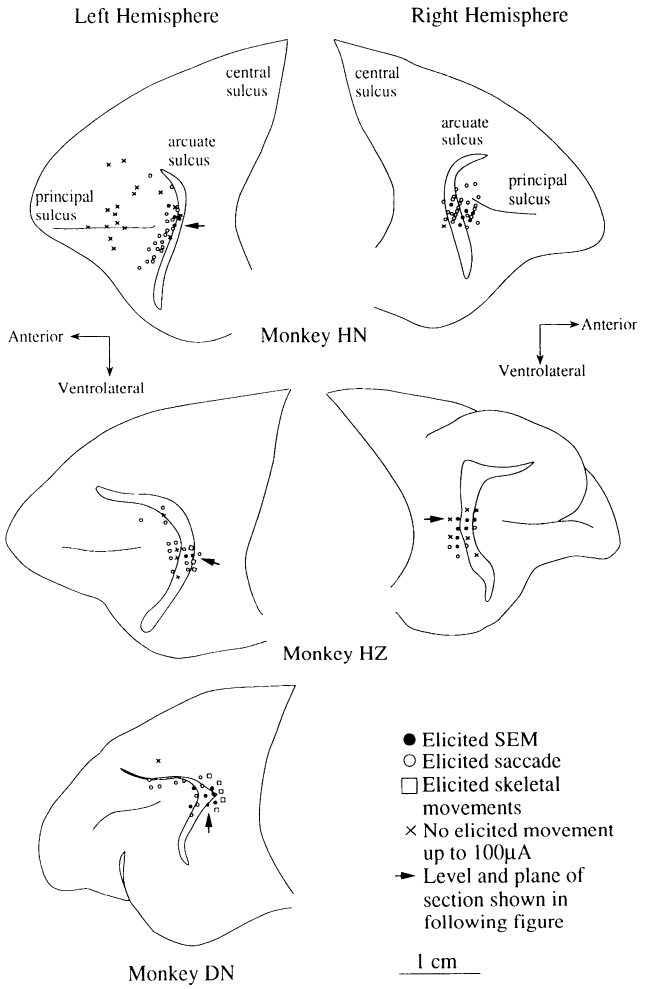

FIG. 8. Location of the periarcuate smooth eye movement (SEM) representation revealed by microstimulation. These dorsolateral views of the frontal lobe show the entry points and the elicited movements of nearly all electrode penetrations made in 5 hemispheres of 3 rhesus monkeys. Maps were reconstructed with reference to the entry points of electrode penetrations directly identified on the basis of iron deposits or marking lesions. SEMs were obtained from a small portion of both arcuate banks, approximately at the level of the principal sulcus. Saccades were obtained mostly from the anterior, and rarely from the posterior arcuate banks, and were often also elicited from sites superficial to those yielding SEMs along the same penetration (these penetrations are marked by ● only). Skeletal movements (of the wrist, forearm, upper arm, shoulder, or face) were elicited at, or immediately posterior to coordinates yielding SEMs. At other locations (marked by ×) stimulation at 100 μA failed to elicit eye movements. The right hemisphere of *monkey HZ* was distorted by a brain edema that developed during recording. For clarity, a few penetrations in *monkey HN's* left hemisphere that yielded no movements or saccades are omitted.

also elicited saccades in other penetrations, at more superficial locations in the same track as that yielding SEMs, or at SEM sites themselves.

Examples of reconstructed electrode penetrations that were marked by iron deposits immediately after eliciting the eye movements are shown in Fig. 9. The planes and locations of the sections outlined are indicated by the arrows in the corresponding hemispheres in Fig. 8. Beneath each section is the averaged SEM obtained at the location identified by lowercase letters in the section. In *monkey HN*, we typically accessed the arcuate fundus at the end of long penetrations along the anterior arcuate bank and often elicited SEMs immediately below low-threshold saccadic sites, as shown in the *top left* panel. In *monkeys HZ* and *DN*, on the other hand, most penetrations coursed through the posterior arcuate bank and appeared to exit the gray matter before reaching the arcuate fundus (last 3 panels). In these monkeys, we elicited SEM with higher currents (75–100 μA) from both superficial and deeper sites in the posterior bank and almost never obtained saccades in the same penetrations. Many penetrations yielding SEMs in these two monkeys entered the cortex immediately anterior to those from which skeletal movements were obtained (Fig. 8). In both arcuate banks, we recorded single neurons responsive during smooth pursuit at or near SEM sites.

Characteristics of anterior and posterior SEM sites

We sought to determine whether the SEM elicited from the arcuate fundus differed from those obtained from the posterior arcuate bank. A small number of stimulation sites were directly localized as illustrated above, on the basis of iron deposits or of marking lesions. The remaining SEM sites were classified as "fundus" sites if they were obtained at the end of penetrations that entered the cortex through the anterior bank and as "posterior bank" sites if their penetrations started above the posterior bank. Although the electrode entry points do not correspond exactly to the locations of sites deeper in the sulcus, this classification is justified by our observations of directly identified penetrations and of electrode marks in the cortex showing that electrode tracks remained within the bank (anterior or posterior) in which they had entered the cortex throughout their lengths. We typically stimulated with currents of ≤50 μA at fundus sites (in *monkey HN*) and with currents of 75–100 μA at posterior bank sites (in *monkeys DN* and *HZ*).

DIRECTIONS. Figure 10 shows the median directions of the same 66 sites used in Fig. 2, now divided into posterior bank sites (n = 35), fundus sites (n = 27), and sites with unidentified locations from the right hemisphere of *monkey DN* (n = 4). Directions of SEMs elicited in the left hemispheres were mirror-reversed to allow grouping of all data points as "contralateral" or "ipsilateral." There was a clear difference between the direction distributions of the fundus and posterior bank sites. The horizontal components of SEMs obtained in the fundus were predominantly ipsilateral, and few of these SEMs had large vertical components. SEMs obtained from the posterior bank, on the other hand, were nearly as often contralateral as ipsilateral, with a much larger proportion having large vertical components. Overall, although ipsilateral SEMs clearly predominated, all movement directions were represented in our sample.

VELOCITIES AND LATENCIES. Because elicited SEM velocity is sensitive to stimulation intensity, the wide range of stimulation intensities used had to be considered in comparing elicited eye velocity across stimulation sites. We used the ratios of eye velocity (obtained in the stationary target condition) to stimulation current as a measure of the "strength" of a site. These ratios did not differ significantly between posterior bank and fundus SEM sites. There were also no differences between the mean latencies of SEM elicited in the fundus and in the posterior bank.

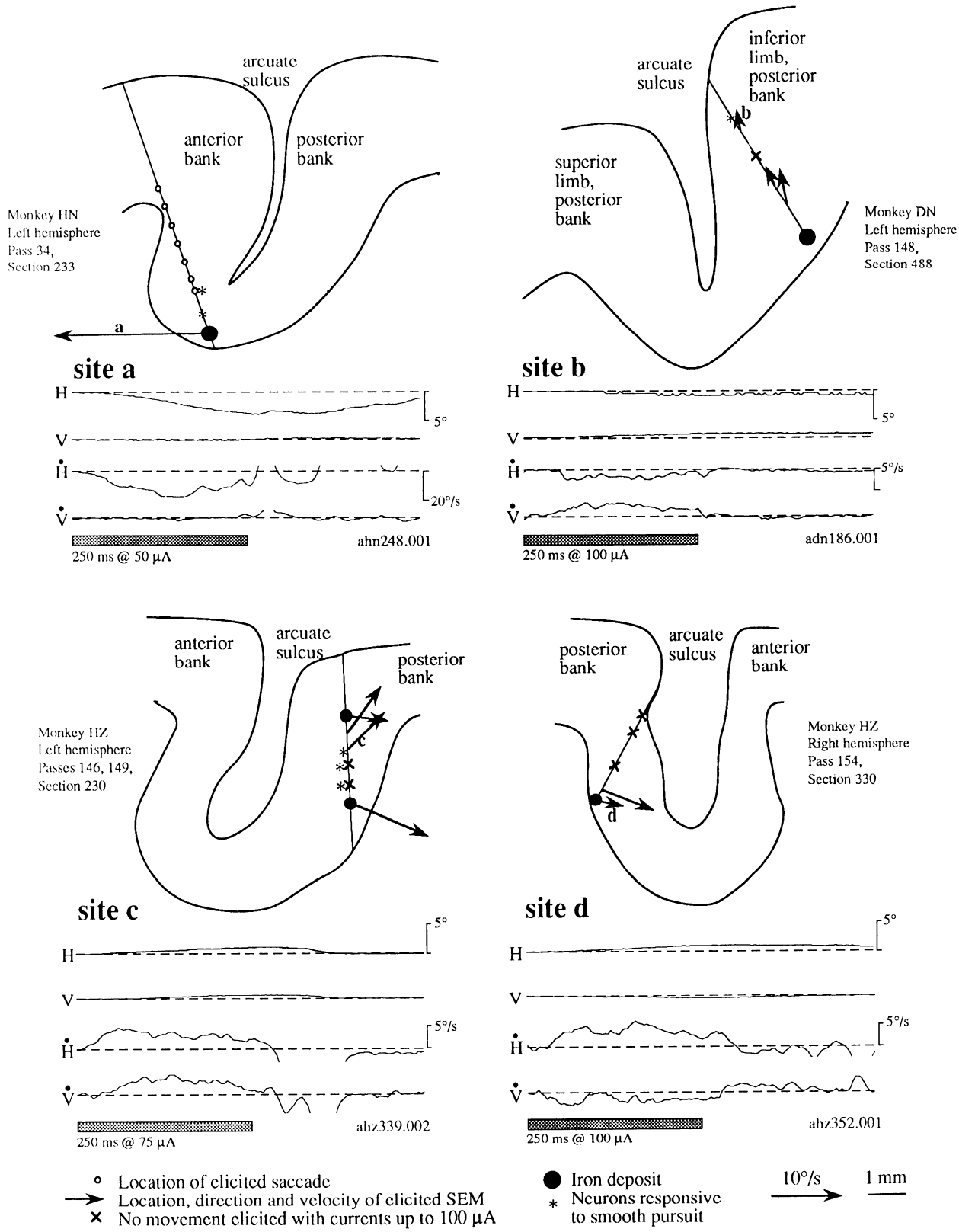

FIG. 9. Smooth eye movements obtained at identified locations. Examples of reconstructed electrode tracks and smooth eye movements obtained in 4 hemispheres are shown. *Top* of each panel: sections shown here are taken at the locations and planes indicated by arrowheads in the corresponding hemispheres in Fig. 8. Note that brains were sectioned approximately perpendicular to the arcuate sulcus at its most posterior point in *monkeys HZ* and *HN* and in the coronal plane in *monkey DN* (note that the section shown for monkey DN, *top right*, cuts through the posteriorly directed "spur" of the arcuate sulcus—see *bottom* of Fig. 8). All physiological data shown are from the same penetration as that on which iron deposits were made; however, in the *bottom left* panel (*monkey HZ*, left hemisphere) data from 2 consecutive penetrations at the same coordinates (each identified by a deposit) are combined. On each track are indicated the locations of saccadic sites (○), the locations and polar dimensions (median peak velocities and median directions) of the elicited smooth eye movement (SEM) (→), sites from which no eye movements were obtained (×), and locations of neurons responsive during smooth pursuit (*). *Bottom* of each panel: averaged eye traces of the SEM identified by the corresponding letter in the section. Traces are, from *top* to *bottom*, horizontal and vertical eye positions (H and V) and eye velocities (Ḣ and V̇). Eye position traces are shown with reference to initial eye position, which varied from site to site and was not always coincident with the center of the screen. Note the different velocity scale used for site a. Other conventions as in Fig. 1.

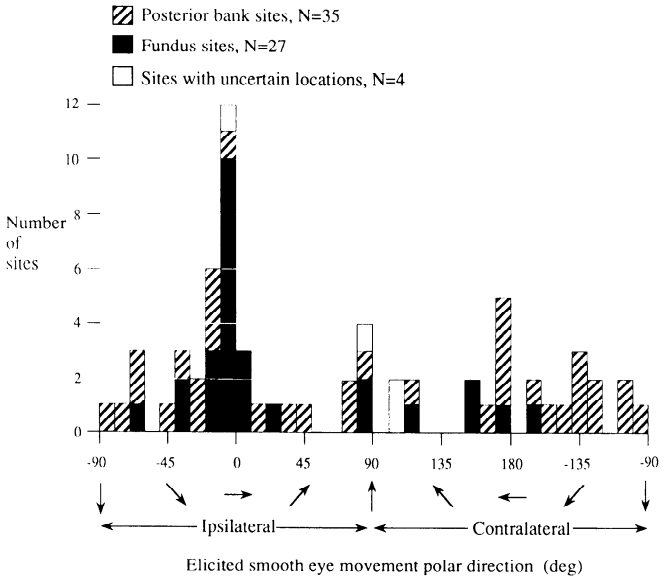

FIG. 10. Elicited smooth eye movement (SEM) directions. The distribution of the median direction of elicited SEM obtained at 66 sites (same records as in Fig. 2) is shown. Directions of SEMs elicited from the right hemisphere are represented in a $-180°-+180°$ convention. Directions of SEMs elicited from the left hemisphere are mirror-reversed, so that all SEMs can be grouped as ipsilateral or contralateral. Note that eye movements elicited from the fundus were predominately ipsilateral, whereas those elicited from the posterior bank were more often directed contralaterally and more often had large vertical components.

Orbital perturbations

At some stimulation sites, the directions of elicited SEM clearly varied as a function of the eyes' orbital position at stimulation onset. Figure 11 shows two-dimensional representations of SEMs elicited from two different sites with different degrees of orbital perturbations. The movements at site HN199 had constant directions over a wide range of initial orbital positions. However, at site HZ067, movements were directed contralaterally (to the left) if the initial eye position was rightward, and ipsilaterally (to the right) if the monkey initially looked leftward. Similarly, their downward components were much diminished as the eye's initial position was lowered.

To quantify these orbital effects, we chose 51 sites where stimulation was tested with a large range of initial eye positions along the horizontal or vertical axis, or both. At each site, we plotted the horizontal and vertical smooth eye excursions during the first 250 ms of stimulation against the respective initial eye coordinates in each trial. We then calculated horizontal and vertical linear-regression coefficients, K_h and K_v, for each site. Because these coefficients were partially dependent on elicited eye velocity, we normalized them by the median velocity components (H_{vel} and V_{vel}) and multiplied the result by 100 for ease of handling. The orbital coefficients thus defined

$$\text{Horizontal coefficient} = 100 * K_h / H_{vel}$$

and

$$\text{Vertical coefficient} = 100 * K_v / V_{vel}$$

are plotted in Fig. 11, *bottom*. Negative coefficients describe negative relationships between initial eye position and elicited velocity (as at site HZ067), positive coefficients correspond to positive relations (as at HN199), and coefficients close to zero indicate little or no orbital effect.

Most orbital coefficients were negative, with means of -1.20 and -0.84 for the horizontal and vertical groups, respectively. Both coefficients were significantly smaller (more negative) for posterior bank than for fundus sites (horizontal coefficients: $t = 2.64$, df $= 45$, $P < 0.02$; vertical coefficients: $t = 2.94$; df $= 33$, $P < 0.01$). Thus orbital position affected SEMs elicited from the posterior bank significantly more than it did those elicited from the arcuate fundus.

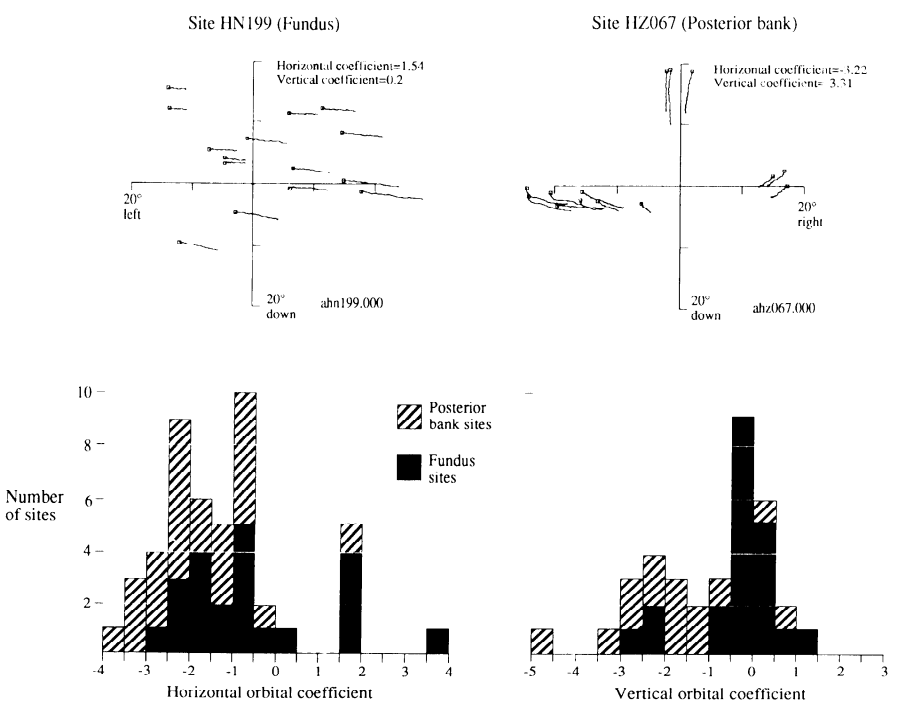

FIG. 11. Orbital perturbations of elicited smooth eye movements (SEMs). *Top*: SEMs elicited from 2 stimulation sites, with different amounts of orbital perturbations. Individual elicited movements are shown on 2-dimensional plots, with eye position at stimulation onset indicated by the small boxes. Site HN199, in the arcuate fundus, was somewhat unusual in having positive orbital coefficients (i.e., rightward and downward eye excursions increased as the eye's initial position was more deviated to the right or down, respectively). Site HZ067 (in the posterior bank) showed a large degree of orbital dependence and had large negative coefficients. *Bottom*: distributions of the horizontal and vertical orbital coefficients of SEMs obtained in the posterior arcuate bank and in the fundus. Note that most horizontal and vertical coefficients are negative, and that coefficients at posterior bank sites tend to be larger (more negative) than those obtained in the fundus.

DISCUSSION

Until recently, it remained unclear whether electrical stimulation of the frontal eye field region could elicit slow eye movements. Several investigators reported that such movements could be elicited from this region in anesthetized rhesus monkeys (Crosby et al. 1952; Wagman 1964) and also in anesthetized marmosets and squirrel monkeys (Blum et al. 1982). However, Robinson and Fuchs (1969), comparing eye movements electrically elicited from awake and anesthetized macaque monkeys, found that intracortical stimulation of the FEF of awake macaques never produced "centering, smooth pursuit or vergence movements or nystagmus" (p. 638). They concluded that elicited ". . . smooth pursuit . . . movements may all be produced by the combination of anesthesia and the large stimulus currents its use necessitates" (p. 641). However, while studying the saccadic FEF, Bruce et al. (1985) elicited SEMs, rather than saccadic eye movements, from several sites in awake macaque monkeys, and noted that these sites lay deep in the arcuate sulcus at or near locations yielding small saccades.

Our results confirm and extend those of Bruce et al. (1985). We elicited slow, continuous eye movements with low-intensity microstimulation (10–100 μA) from a total of 86 sites in six hemispheres tested. Because these SEMs were elicited while the monkey's eyes were stationary, usually fixating a target light, they are neither ocular drifts nor slow saccades sometimes elicited during light sleep. These SEMs, elicited from a small portion of the arcuate fundus and neighboring posterior bank approximately at the level of the principal sulcus, seem to define a discrete, functionally distinct region between the saccadic FEF and premotor cortex (area 6).

Significance of elicited SEMs

Several recent experimental lesion studies have revealed the importance of the FEF for smooth pursuit eye movements. Comparisons of our findings with these reports strongly suggest that the elicited SEMs represent a physiological involvement of the periarcuate region in smooth pursuit rather than in other types of slow eye movements, such as the slow phases of the optokinetic or vestibular reflexes, or unphysiological movements. Monkeys with FEF lesions can suffer lasting impairments in smooth pursuit gain and in their abilities to predictively initiate or continue smooth tracking (Keating 1991; Lynch 1987, 1989; MacAvoy et al. 1991). In agreement with the location of the SEM region defined by microstimulation—ventral and posterior to the saccadic FEF—pursuit deficits are not obtained with FEF lesions confined to the lip and anterior bank of the arcuate sulcus that spare its fundus and posterior bank (MacAvoy et al. 1991). In fact, this buried location may explain why previous physiological and lesion studies did not locate a smooth pursuit representation in the FEF (e.g., Robinson and Fuchs 1969; Schiller and Logothetis 1987). The SEMs we elicited from this region were mostly ipsilateral, consistent with the predominantly ipsilateral tracking deficits produced by unilateral lesions of both the monkey and human FEF (MacAvoy and Bruce 1989; MacAvoy et al. 1991; Morrow and Sharpe 1990a,b; but see Keating 1991). Finally, neurons recorded at periarcuate SEM sites respond in relation to smooth pursuit but not saccadic eye movements (present results; Bruce et al. 1985; Gottlieb et al. 1989, 1991). Moreover, their responses often start before the pursuit movements, and their best tracking directions correlate with the directions of the SEMs elicited from the same site (Gottlieb et al. 1991).

Coding of SEM direction and amplitude

The initial accelerations and the peak velocities of elicited SEMs usually increased with current intensity at a given stimulation site, whereas their directions remained independent of current intensity, characteristic only of the stimulation location. These findings suggest that smooth pursuit acceleration or velocity are coded by the intensity of neural activity, whereas pursuit direction is coded by the location of neural activity ("rate" and "place" codes, respectively). This organization differs from the saccadic FEF, where both saccade directions and amplitudes are specified in place codes (Robinson and Fuchs 1969). Along with other observations, the place representation of saccades has been cited in support of the notion that the FEF acts primarily as a trigger for saccades, only specifying the overall movement metric and not other details such as its acceleration, velocity, duration, or trajectory (Bruce 1990). In contrast, the SEM region may participate continuously in the specification of the acceleration, velocity, and duration of the pursuit movements.

Acceleration versus velocity signals

To initiate slow eye movements from stationary fixation, the microstimulation may have signaled either an eye velocity goal or an instantaneous eye acceleration. The velocity goal hypothesis predicts that the eye will reach a plateau velocity and maintain it throughout the stimulation train. The acceleration hypothesis, on the other hand, predicts the eye will continue accelerating for all or most of the stimulation train.

Stimulation in the presence of a stationary fixation target (closed-loop conditions) typically caused the eye to reach a plateau velocity and maintain it throughout the stimulation, apparently supporting the former hypothesis. However, when the fixation target was stabilized on the fovea, thus eliminating the retinal slip it had produced in the closed-loop condition, the eye continued to accelerate for as long as the stimulation train was applied. The resulting increase in eye velocity in the stabilized relative to the nonstabilized condition started $\sim$100 ms after stimulation onset, close to the estimated visual latency of the pursuit system. These results suggest that the FEF stimulation triggers an eye acceleration signal, and that this signal can be modified by visual signals before effecting the eye movement.

The triggering of an acceleration signal by cortical stimulation is consistent with models that postulate that the smooth pursuit command is elaborated in a series of successive transformations of retinal error signals (Goldreich et al. 1992; Lisberger et al. 1987). Drawing from analyses of visually guided pursuit (e.g., Lisberger et al. 1981), these models propose that retinal signals, mainly velocity errors (differences between target and eye velocities), but also ac-

celeration and position errors, are translated rather directly into smooth eye accelerations appropriate for correcting these errors. The acceleration signals are then integrated twice to obtain first a representation of smooth eye velocity and then one of eye position, and summed position and velocity commands are relayed to motor neurons. We postulate that the FEF participates in the first of these transformations, the derivation of smooth eye acceleration from visual information and from task demands. The position of the FEF in the brain's smooth pursuit network is consistent with this hypothesis. Thus the FEF lies downstream from the middle temporal (MT) and medial superior temporal (MST) areas thought to provide most of the visual information for smooth pursuit, and it lies upstream from pontocerebellar and brain stem circuits believed to effect the acceleration-to-velocity and velocity-to-position integrations (for reviews, see Eckmiller 1987; Keller and Heinen 1991; Lisberger et al. 1987).

Alternative smooth pursuit models propose that an internal representation of eye velocity is added to the retinal slip signal, constructing a representation of target velocity with respect to the head relatively early in the pursuit system (e.g., Robinson et al. 1986; Yasui and Young 1975). This target velocity signal is then used as an eye velocity goal for the smooth pursuit controller. On the basis of their findings that pursuit responses of MST neurons persist in the absence of retinal slip, Newsome et al. (1988) postulated that such a target velocity representation may be found in the MST. As discussed above, we do not think that electrical stimulation of the FEF mimics an eye velocity goal; however, the acceleration signal provided by the FEF could serve as an additional input to models of this type.

Stimulation in MT and MST produces eye accelerations during ongoing pursuit movements, but, unlike FEF stimulation, generally does not evoke slow eye movements from stationary fixation. Also unlike FEF stimulation, smooth eye accelerations evoked from MT and MST are insensitive to concomitant retinal slip (Komatsu and Wurtz 1989). These differences suggest that electrical stimulation of MT and MST activates primarily a visual motion signal, and that it can "take over," or block the visual input pathway, thus temporarily disconnecting retinal signals from the pursuit system (Komatsu and Wurtz 1989). In contrast, electrical stimulation of the FEF leaves open the pursuit system's visual feedback pathway. Thus the FEF seems to be one stage removed from MT and MST and to encode not a purely visual, but an oculomotor acceleration signal. This signal may combine with visual motion information in the dorsolateral pontine nucleus (DLPN) or in the nucleus reticularis tegmenti pontis (nRTP), where neurons respond to passive visual motion in addition to their pursuit responses (Keller and Crandall 1983; Mustari et al. 1988).

Orbital perturbations of elicited SEM

At some stimulation sites, the directions of elicited SEMs varied as a function of initial eye positions, sometimes appearing to converge toward a particular "orbital goal." Orbital effects apparently similar to the ones we report were described for SEMs elicited from the nRTP (Yamada et al. 1991) and from the cerebellum (Ron and Robinson 1973). This phenomenon also seems analogous with the orbital effects reported for elicited saccades in several structures (e.g., Bruce 1990; Schlag and Schlag-Rey 1990).

A possible interpretation of these effects is that neurons at some stimulation sites specify an orbital goal, or end point for pursuit, rather than a pursuit vector. However, this interpretation is difficult to reconcile with the primary function of the pursuit system—to accurately match eye velocity to target velocity independently of orbital location. Thus pursuit neurons in the nRTP and cerebellum are conceived of as coding pursuit direction, despite the orbital effects on elicited SEMs mentioned above. These perturbations may reflect stimulation artifacts, such as conjoint activation of neurons that are not normally synchronously active, or engagement of the pursuit system in an unbalanced or nonphysiological pattern. Alternatively, they may be related to the gaze-related neural activity observed in the FEF (Bizzi 1968; Bruce and Goldberg 1985) that often coexists with pursuit responses in single neurons (Gottlieb et al. 1989, 1991). A final distinction among these possibilities must be based on analysis of the gaze- and pursuit-related neuronal responses in this region.

The orbital effects were greater at sites located in the posterior bank than at those in the arcuate fundus. Although it is possible that posterior and fundal pursuit neurons have distinct functions and efferent targets, we cannot rule out the possibility that this difference was simply due to the higher stimulation currents used at posterior bank relative to fundus sites.

Connections mediating the elicited SEMs

As mentioned above, the main pathway for smooth pursuit is thought to comprise projections from several neocortical areas (striate cortex, MT, MST, and FEF) to the pons and from there to the cerebellum (for reviews see Eckmiller 1987; Keller and Heinen 1991; Lisberger et al. 1987; Tusa and Ungerleider 1988). The periarcuate cortex (including both arcuate banks) most likely can influence smooth pursuit through its projections to the pontine nuclei, especially to the DLPN and to the nRTP (Huerta et al. 1986; Leichnetz et al. 1984b; Stanton et al. 1988). The DLPN contains neurons responsive during smooth pursuit (Mustari et al. 1988), its microstimulation causes smooth eye accelerations (May et al. 1985), and small chemical lesions cause ipsilateral pursuit deficits (May et al. 1988). The nRTP has been implicated in smooth pursuit on the basis of similar evidence (Suzuki et al. 1990, 1991; Yamada et al. 1991). The DLPN and nRTP project to the flocculus and to the oculomotor vermis of the cerebellum (Langer et al. 1985; Yamada and Noda 1987), both known to be crucial for pursuit (Lisberger and Fuchs 1978; Ron and Robinson 1973; Stone and Lisberger 1990; Suzuki and Keller 1988; Zee et al. 1981). Finally, both arcuate banks project to the paramedian pontine reticular formation (PPRF; Leichnetz et al. 1984b; Schnyder et al. 1985), whose microstimulation produces SEMs similar in appearance to FEF SEMs (Cohen and Komatsuzaki 1972; Keller 1974). However, the slow eye movements elicited from the PPRF may not

represent a specific engagement of the smooth pursuit system, but rather a direct activation of the neural integrator used by all the eye movement systems.

The latency of SEMs evoked from the FEF, ~40 ms, is consistent with a transcerebellar pathway, because SEMs elicited from the cerebellum have shorter latencies of ~15 ms (Ron and Robinson 1973). Smooth eye velocities obtained from the cerebellum are similar to the ones we obtain, typically 12–15°/s (Belknap and Noda 1987; Ron and Robinson 1973).

The SEMs elicited from FEF are similar to those obtained from the nRTP and the cerebellum in that they can be evoked from stationary eye positions, with or without fixation of a visual target (Ron and Robinson 1973; Yamada et al. 1991). In contrast, as mentioned above, microstimulation of the DLPN and of MT and MST can produce eye accelerations during ongoing smooth pursuit but usually cannot initiate slow movements from stationary fixation (Komatsu and Wurtz 1989; May et al. 1985). Thus these arcuate and superior temporal areas may access the pursuit system through two partially independent pathways, the former relying mainly on the nRTP and the latter mainly on the DLPN. This parallel organization has been proposed to explain the findings of significant recovery in pursuit deficits after lesions of MT, MST, DLPN, and nRTP (Keller and Heinen 1991; Suzuki et al. 1990, 1991).

The finding that slow eye movements can be elicited from the posterior arcuate bank was surprising because this area is traditionally linked to, and studied in the context of, skeletal and not ocular movements (for review, see Wise 1985). However, our findings are consistent with previous reports of eye movements elicited from the posterior arcuate bank in anesthetized owl, squirrel, and marmoset monkey (Blum et al. 1982; Preuss et al. 1991) and in awake rhesus monkey (Segraves and Goldberg 1987). Furthermore, as mentioned above, posterior arcuate cortex has efferents to the pontine nuclei, to the nRTP (Leichnetz et al. 1984b), and to the paraoculomotor complex (Leichnetz et al. 1984a), which may have directly mediated elicited SEMs. Interestingly, Rizzolatti et al. (1983) reported that removal of the posterior arcuate bank produces deficits in eye-head coordination during smooth pursuit.

Microstimulation of cortical, pontine, and cerebellar structures involved in smooth pursuit evokes predominantly ipsilateral SEMs (Komatsu and Wurtz 1989; May et al. 1985; Ron and Robinson 1973), suggesting that the main pathways for pursuit are ipsilateral and noncrossed. The main component of the periarcuate pontine projection is ipsilateral (Huerta et al. 1986; Stanton et al. 1988) and probably mediated the ipsilateral SEMs in our sample. However, the FEF and the premotor area project bilaterally to the nRTP (Huerta et al. 1987; Leichnetz et al. 1984b; Stanton et al. 1988), and the decussating branch of this projection may have mediated the contralateral SEMs. In addition, the higher stimulation intensities we used in the posterior bank may have elicited contralateral SEMs by activating projections to the contralateral periarcuate region.

We thank G. Leydon for providing computer programs used for data analysis and illustration.

This work was supported by National Institutes of Health Grants EY-04740 and MH-44866.

Address reprint requests to C. J. Bruce.

Received 6 July 1992; accepted in final form 22 October 1992.

REFERENCES

BELKNAP, D. B. AND NODA, H. Eye movements evoked by microstimulation in the flocculus of the alert macaque. *Exp. Brain Res.* 67: 352–362, 1987.

BIZZI, E. Discharge of frontal eye field neurons during saccadic and following eye movements in unanesthetized monkeys. *Exp. Brain Res.* 6: 69–80, 1968.

BLUM, B., KULIKOWSKI, J. J., CARDEN, D., AND HARWOOD, D. Eye movements induced by electrical stimulation of the frontal eye fields of marmosets and squirrel monkeys. *Brain Behav. Evol.* 21: 34–41, 1982.

BRUCE, C. J. Integration of sensory and motor signals for saccadic eye movements in the primate frontal eye fields. In: *Signal and Sense, Local and Global Order in Perceptual Maps*, edited by G. M. Edelman, W. E. Gall, and W. M. Cowan. New York: Wiley, 1990, p. 261–314.

BRUCE, C. J. AND BORDEN, J. A. The primate frontal eye fields are necessary for predictive saccadic tracking. *Soc. Neurosci. Abstr.* 12: 1086, 1986.

BRUCE, C. J. AND GOLDBERG, M. E. Primate frontal eye fields. I. Single neurons discharging before saccades. *J. Neurophysiol.* 53: 606–635, 1985.

BRUCE, C. J., GOLDBERG, M. E., BUSHNELL, M. C., AND STANTON, G. B. Primate frontal eye fields. II. Physiological and anatomical correlates of electrically evoked eye movements. *J. Neurophysiol.* 54: 714–734, 1985.

COHEN, B. AND KOMATSUZAKI, A. Eye movements induced by stimulation of the pontine reticular formation: evidence for integration in oculomotor pathways. *Exp. Neurol.* 36: 101–117, 1972.

CRIST, C. F., YAMASAKI, D. S. G., KOMATSU, H., AND WURTZ, R. H. A grid system and a microsyringe for single cell recording. *J. Neurosci. Methods* 26: 117–122, 1988.

CROSBY, E. C., YOSS, R. E., AND HENDERSON, J. W. The mammalian midbrain and isthmus regions. II. The fiber connections. D. The pattern for eye movements on the frontal eye field and the discharge of specific portions of this field to and through midbrain levels. *J. Comp. Neurol.* 97: 357–383, 1952.

DENG, S.-Y., GOLDBERG, M. E., SEGRAVES, M. A., UNGERLEIDER, L. G., AND MISHKIN, M. The effect of unilateral ablation of the frontal eye fields on saccadic performance in the monkey. In: *Adaptive Processes in Visual and Oculomotor Systems*, edited by E. L. Keller and D. S. Zee. Oxford, UK: Pergamon, 1986, p. 201–208.

ECKMILLER, R. Neural control of pursuit eye movements. *Physiol. Rev.* 67: 797–857, 1987.

GOLDREICH, D., KRAUZLIS, R. J., AND LISBERGER, S. G. Effect of changing feedback delay on spontaneous oscillations in smooth pursuit eye movements of monkeys. *J. Neurophysiol.* 67: 625–638, 1992.

GOTTLIEB, J. P., MACAVOY, M. G., AND BRUCE, C. J. Unit activity related to smooth pursuit eye movements in rhesus monkey frontal eye fields. *Soc. Neurosci. Abstr.* 15: 1203, 1989.

GOTTLIEB, J. P., MACAVOY, M. G., AND BRUCE, C. J. Smooth eye movements elicited from the monkey peri-arcuate area: topography and relation to single unit responses. *Soc. Neurosci. Abstr.* 17: 544, 1991.

HUERTA, M. F., KRUBITZER, L. A., AND KAAS, J. H. Frontal eye field as defined by intracortical microstimulation in squirrel monkeys, owl monkeys, and macaque monkeys. I. Subcortical connections. *J. Comp. Neurol.* 253: 415–439, 1986.

HUERTA, M. F., KRUBITZER, L. A., AND KAAS, J. H. Frontal eye field as defined by intracortical microstimulation in squirrel monkeys, owl monkeys, and macaque monkeys. II. Cortical connections. *J. Comp. Neurol.* 265: 332–361, 1987.

JUDGE, S. J., RICHMOND, B. J., AND CHU, F. C. Implantation of magnetic search coils for measurement of eye position: an improved method. *Vision Res.* 20: 535–538, 1980.

KEATING, E. G. Frontal eye field lesions impair predictive and visually-guided pursuit eye movements. *Exp. Brain Res.* 86: 311–323, 1991.

KELLER, E. L. Participation of medial pontine reticular formation movement generation in monkey. *J. Neurophysiol.* 37: 316–332, 1974.

KELLER, E. L. AND CRANDALL, W. F. Neuronal responses to optokinetic stimuli in pontine nuclei of behaving monkey. *J. Neurophysiol.* 49: 169–187, 1983.

KELLER, E. L. AND HEINEN, S. J. Generation of smooth-pursuit eye movements: neuronal mechanisms and pathways. *Neurosci. Res.* 11: 79–107, 1991.

KOMATSU, H. AND WURTZ, R. H. Modulation of pursuit eye movements by stimulation of cortical areas MT and MST. *J. Neurophysiol.* 62: 31–47, 1989.

LANGER, T., FUCHS, A. F., SCUDDER, C. A., AND CHUBB, M. C. Afferents to the flocculus of the cerebellum of the rhesus macaque as revealed by retrograde transport of horseradish peroxidase. *J. Comp. Neurol.* 235: 1–25, 1985.

LATTO, R. The effects of bilateral frontal eye-field lesions on the learning of a visual search task by rhesus monkeys. *Brain Res.* 147: 370–376, 1978.

LEICHNETZ, G. R., SPENCER, R. F., AND SMITH, D. J. Cortical projections to nuclei adjacent to the oculomotor complex in the medial dienmesencephalic tegmentum in the monkey. *J. Comp. Neurol.* 228: 359–387, 1984a.

LEICHNETZ, G. R., SMITH, D. J., AND SPENCER, R. F. Cortical projections to the paramedian tegmental and basilar pons in the monkey. *J. Comp. Neurol.* 228: 388–408, 1984b.

LISBERGER, S. G., EVINGER, C., JOHANSON, G. W., AND FUCHS, A. F. Relationship between eye acceleration and retinal image velocity during foveal smooth pursuit in man and monkey. *J. Neurophysiol.* 46: 229–249, 1981.

LISBERGER, S. G. AND FUCHS, A. F. Role of primate flocculus during rapid behavioral modification of vestibulo-ocular reflex. I. Purkinje cell activity during visually guided horizontal smooth pursuit eye movements and passive head rotation. *J. Neurophysiol.* 41: 733–763, 1978.

LISBERGER, S. G., MORRIS, E. J., AND TYCHSEN, L. Visual motion processing and sensory-motor integration for smooth pursuit eye movements. *Annu. Rev. Neurosci.* 10: 97–130, 1987.

LYNCH, J. C. Frontal eye field lesions in monkeys disrupt visual pursuit. *Exp. Brain Res.* 68: 437–444, 1987.

LYNCH, J. C. Pursuit recovery after frontal eye field lesions in monkeys. *Soc. Neurosci. Abstr.* 15: 1202, 1989.

LYNCH, J. C., ALLISON, J. C., HINES, R. S., AND ROARK, R. L. Oculomotor impairment following combined lesions of parieto-occipital cortex and frontal eye fields in rhesus monkeys. *Soc. Neurosci. Abstr.* 12: 1806, 1986.

MACAVOY, M. G. AND BRUCE, C. J. Oculomotor deficits associated with lesions of the frontal eye field area in macaque monkeys. *Soc. Neurosci. Abstr.* 15: 1203, 1989.

MACAVOY, M. G., BRUCE, C. J., AND GOTTLIEB, J. P. Smooth eye movements elicited by microstimulation in the frontal eye fields region of alert macaque monkeys. *Soc. Neurosci. Abstr.* 14: 956, 1988.

MACAVOY, M. G., GOTTLIEB, J. P., AND BRUCE, C. J. Smooth pursuit eye movement representation in the primate frontal eye field. *Cerebral Cortex* 1: 95–102, 1991.

MAUNSELL, J. R. AND VAN ESSEN, D. C. Functional properties of neurons in middle temporal visual area of the macaque monkey. I. Selectivity for stimulus direction, speed and orientation. *J. Neurophysiol.* 49: 1127–1147, 1983.

MAY, J. G., KELLER, E. L., AND CRANDALL, W. F. Changes in eye velocity during smooth-pursuit tracking induced by microstimulation in the dorsolateral pontine nucleus of the monkey. *Soc. Neurosci. Abstr.* 11: 79, 1985.

MAY, J. G., KELLER, E. L., AND SUZUKI, D. A. Smooth-pursuit eye movement deficits with chemical lesions in the dorsolateral pontine nucleus of the monkey. *J. Neurophysiol.* 59: 952–977, 1988.

MORROW, M. J. AND SHARPE, J. A. Cerebral hemispheric localization of smooth pursuit asymmetry. *Neurology* 40: 284–292, 1990a.

MORROW, M. J. AND SHARPE, J. A. Ocular tracking in patients with frontal lobe lesions. *Soc. Neurosci. Abstr.* 16: 899, 1990b.

MUSTARI, M. J., FUCHS, A. F., AND WALLMAN, J. Response properties of dorsolateral pontine units during smooth pursuit in the rhesus macaque. *J. Neurophysiol.* 60: 664–686, 1988.

NEWSOME, W. T., WURTZ, R. H., AND KOMATSU, H. Relation of cortical areas MT and MST to pursuit eye movements. II. Differentiation of retinal from extraretinal inputs. *J. Neurophysiol.* 60: 604–620, 1988.

PREUSS, T. M., STEPNIEWSKA, I., AND KAAS, J. H. Microstimulation studies of premotor and oculomotor cortex in owl monkeys. *Soc. Neurosci. Abstr.* 17: 1022, 1991.

RIZZOLATTI, G., MATELLI, M., AND PAVESI, G. Deficits in attention and movement following the removal of postarcuate (area 6) and prearcuate (area 8) cortex in macaque monkeys. *Brain* 106: 655–673, 1983.

ROBINSON, D. A. A method of measuring eye movements using a scleral search coil in a magnetic field. *IEEE Trans. Biomed. Eng.* 10: 137–145, 1963.

ROBINSON, D. A. AND FUCHS, A. F. Eye movements evoked by stimulation of frontal eye fields. *J. Neurophysiol.* 32: 637–648, 1969.

ROBINSON, D. A., GORDON, J. L., AND GORDON, S. E. A model of the smooth pursuit eye movement system. *Biol. Cybern.* 55: 43–57, 1986.

RON, S. AND ROBINSON, D. A. Eye movements evoked by cerebellar stimulation in the alert monkey. *J. Neurophysiol.* 36: 1004–1022, 1973.

SCHILLER, P. H. AND LOGOTHETIS, N. K. The effect of frontal eye field and superior colliculus lesions on the saccadic and pursuit eye movement initiation. *Soc. Neurosci. Abstr.* 13: 1092, 1987.

SCHILLER, P. H., TRUE, S. D., AND CONWAY, J. L. Deficits in eye movements following frontal eye-field and superior colliculus ablations. *J. Neurophysiol.* 44: 1175–1189, 1980.

SCHLAG, J. AND SCHLAG-REY, M. Colliding saccades may reveal the secret of their marching orders. *Trends Neurosci.* 13: 410–415, 1990.

SCHNYDER, H., REISINE, H., HEPP, K., AND HENN, V. The frontal eye field projection to the paramedian pontine reticular formation traced with wheat germ agglutinin in the monkey. *Brain Res.* 329: 151–160, 1985.

SEGRAVES, M. A. AND GOLDBERG, M. E. Functional properties of corticotectal neurons in the monkey's frontal eye field. *J. Neurophysiol.* 58: 1387–1419, 1987.

SEGRAVES, M. A., GOLDBERG, M. E., DENG, S., BRUCE, C. J., UNGERLEIDER, L. G., AND MISHKIN, M. The role of striate cortex in the guidance of eye movements. *J. Neurosci.* 7: 3040–3058, 1987.

STANTON, G. B., DENG, S.-Y., GOLDBERG, M. E., AND MCMULLEN, N. T. Cytoarchitectural characteristics of the frontal eye fields in macaque monkeys. *J. Comp. Neurol.* 282: 415–427, 1989.

STANTON, G. B., GOLDBERG, M. E., AND BRUCE, C. J. Frontal eye field efferents in the macaque monkey. II. Topography of terminal fields in midbrain and pons. *J. Comp. Neurol.* 271: 493–506, 1988.

STONE, L. S. AND LISBERGER, S. G. Visual responses of Purkinje cells in the cerebellar flocculus during smooth pursuit eye movements in monkeys. I. Simple spikes. *J. Neurophysiol.* 63: 1241–1261, 1990.

SUZUKI, D. A. AND KELLER, E. L. The role of the posterior vermis of monkey cerebellum in smooth-pursuit eye movement control. I. Eye and head movement-related activity. *J. Neurophysiol.* 59: 1–18, 1988.

SUZUKI, D. A., YAMADA, T., BETELAK, K. F., AND YEE, R. D. Smooth-pursuit eye movement related activity in monkey nucleus reticularis tegmenti pontis. *Soc. Neurosci. Abstr.* 17: 459, 1991.

SUZUKI, D. A., YEE, R. D., AND BETELAK, K. Deficits in smooth-pursuit eye movements following lidocaine injection in monkey nucleus reticularis tegmenti pontis (NRTP). *Soc. Neurosci. Abstr.* 16: 903, 1990.

TUSA, R. J. AND UNGERLEIDER, L. G. Fiber pathways of cortical areas mediating smooth pursuit eye movements in monkeys. *Ann. Neurol.* 23: 174–183, 1988.

WAGMAN, I. H. Eye movements induced by electric stimulation of cerebrum in monkeys and their relationship to bodily movements. In: *The Oculomotor System*, edited by M. B. Bender. New York: Harper & Row, 1964, p. 18–39.

WISE, S. P. The primate premotor cortex: past, present and preparatory. *Annu. Rev. Neurosci.* 8: 1–19, 1985.

YAMADA, J. AND NODA, H. Afferent and efferent connections of the oculomotor cerebellar vermis in the macaque monkey. *J. Comp. Neurol.* 265: 224–241, 1987.

YAMADA, T., SUZUKI, D. A., BETELAK, K. F., AND YEE, R. D. Initial eye position dependence of eye movements evoked by microstimulation in the monkey nucleus reticularis tegmenti pontis. *Soc. Neurosci. Abstr.* 17: 459, 1991.

YASUI, S. AND YOUNG, R. L. Perceived visual motion as effective stimulus to pursuit eye movement system. *Science Wash. DC* 190: 906–908, 1975.

ZEE, D. S., YAMASAKI, A., BUTLER, P. H., AND GUCER, G. Effect of ablation of flocculus and paraflocculus on eye movement in primate. *J. Neurophysiol.* 46: 878–899, 1981.